Desalination and Water Treatment
www.deswater.com

doi: 10.5004/dwt.2017.21562

92 (2017) 267–274
October

Removal of lead ions from aqueous solutions using novel-modified magnetic nanoparticles: optimization, isotherm, and kinetics studies

S. Jafarinejad[a,*], M. Faraji[b], P. Jafari[a], J. Mokhtari-Aliabad[c]

[a]*Chemical Engineering Division, College of Environment, UoE, Karaj, Iran, Tel. +982632803027 Ext. 147; emails: jafarinejad83@gmail.com (S. Jafarinejad), parisa.jafari991@gmail.com (P. Jafari)*
[b]*Faculty of Food Industry and Agriculture, Department of Food Science and Technology, Standard Research Institute (SRI), P.O. Box 31745-139, Karaj, Iran, email: mfaraji@standard.ac.ir*
[c]*Department of Chemistry, Science and Research Branch, Islamic Azad University, Tehran, Iran, email: j.mokhtari@modares.ac.ir*

Received 29 November 2016; Accepted 30 July 2017

ABSTRACT

Lead pollution can cause a variety of environmental and health concerns. In this research, a novel sulfur-modified magnetic nanoparticle was synthesized and applied as an adsorbent for the removal of lead (Pb^{2+}) ions from aqueous solutions. The adsorbent was characterized by scanning electron microscopy, Fourier transform infrared spectroscopy, and thermogravimetric analysis. Effect of pH, adsorbent dosage, contact time, and initial concentration of Pb^{2+} on the removal efficiency were investigated and optimized. The equilibrium data were well fitted to the Langmuir isotherm model and the maximum monolayer capacity (q_m) was obtained 14.03 mg g^{-1}. Also, adsorption kinetic data were well explained by pseudo-second-order kinetic model. The desorption efficiency was approximately 98% which this desorption ability of the adsorbent can diminish operation costs and may indicate industrial applicability. Under optimum conditions, the applicability of the adsorbent in real wastewater sample was investigated by removal of lead from effluent wastewater from a battery factory wastewater treatment plant in which the removal efficiency was 76.72%.

Keywords: Lead; Health concerns; Magnetic nanoparticles; Adsorption; Removal

1. Introduction

There are considerable attentions to the pollution of the environment by heavy metals. Heavy metals are essentially non-biodegradable in the environment and can accumulate in living tissues especially in human bodies causing various diseases and disorders [1,2]. Depending on the metal, its concentration, route of exposure, as well as the age, genetics, and nutritional status of exposed targets, heavy metals can have a variety of environmental and health concerns [3,4].

Lead (Pb^{2+}) is applied in industrial manufacturing processes such as metal plating, as well as in batteries for energy storage. Problem of lead pollution is originated from the waste streams from these uses as well as vehicular fuel combustion and emissions [5,6]. Pb^{2+} ions can accumulated in body tissues by long-term exposure to low concentration level due to the rather slow rate of excretion [2]. Extended exposure of the human body to Pb^{2+} ions in the environment may cause nausea, convulsions, anemia, renal failure, and cancer, even if the concentration of Pb^{2+} ions is very low [5,7]. Pb^{2+} also exhibits strong neurotoxicity [5,8]. Pregnant women and children can particularly vulnerable to the toxic effects of Pb^{2+} ions due to its impacts on the growth of the brain and nervous system [5,9]. In addition, Pb^{2+} ion is very difficult to eliminate once it enters the body, and causes permanent damage [5,10]. Maximum contamination levels for Pb^{2+} in sludge (soil), drinking water, and supporting aquatic life regulated by United States Environmental Protection Agency (US EPA) are 420 mg kg^{-1}, 0.01 mg L^{-1}, and 0.0058 mg L^{-1}, respectively [3,11]. Thus, it is essential to take considerable effort for

* Corresponding author.

developing effective treatment techniques for removal of Pb^{2+} ions from wastewater before its discharge into the near water bodies [12].

Adsorption is an efficient technique for the removal and separation of heavy metal ions [5,13]. In recent years, magnetic nanoparticles (MNPs) as an efficient adsorbent with the large specific surface area and small diffusion resistance have been recognized and introduced [2,14,15]. In general, the MNPs with affinity to target species can be readily isolated from sample solutions using an external magnetic field without additional separation steps such as filtration or centrifugation [2].

Up to date, MNPs have been applied as adsorbents for the separation and removal of metals such as Pb^{2+} from aqueous solutions. For example, Lu et al. [5] prepared a novel magnetic carboxylated cellulose nanocrystal composite (CCN-Fe_3O_4) as an adsorbent for the adsorption of Pb^{2+} from aqueous solution and reported that Pb^{2+} adsorption onto CCN-Fe_3O_4 reached equilibrium in 240 min, and the maximum adsorption capacity of Pb^{2+} was 63.78 mg g^{-1} at 298.2 K. Afzali and Fayazi [2] concluded that the magnetic halloysite nanotubes@manganese oxide (MHNTs@MnO_2) nanocomposite is an effective material for the removal of Pb^{2+} from aqueous solutions. Rajput et al. [16] synthesized magnetic magnetite (Fe_3O_4) nanoparticle by chemical co-precipitation and used it for successful removal of Cr^{6+} and Pb^{2+} from aqueous solutions in batch experiment. Maximum Cr^{6+} and Pb^{2+} removal occurred at pH 2.0 and 5.0, respectively, and maximum Langmuir adsorption capacities were 34.87 mg g^{-1} (Cr^{6+}) and 53.11 mg g^{-1} (Pb^{2+}) at 45°C. Verma et al. [17] functionalized the magnetic Fe_3O_4 nanoparticles with glycine at pH 6. Then, they entrapped the glycine-functionalized magnetic nanoparticles into alginate polymer as beads and used as adsorbent for the removal of Pb^{2+} ions. They reported that 92.8% Pb^{2+} could be removed just in 10 min and the adsorbent could be regenerated four times simply by 0.2 M HNO_3 retaining 90% of the adsorption capacity [17]. Lingamdinne et al. [18] synthesized magnetic inverse spinel iron oxide nanoparticles (MISFNPs) using a biogenic methodology and found that the adsorption of Pb^{2+} and Cr^{3+} on nanoparticles followed an endothermic process. They concluded that MISFNPs synthesized by a green route is capable of recycling and removal of heavy metals without loss of its stability [18]. Beyki et al. [19] investigated green synthesis of Fe_3O_4 nanoparticles as a magnetic core to prepare poly(1,4–phenylenediamine) nanocomposite and used this magnetic polymer nanocomposite as an adsorbent in the removal of Pb^{2+} ions and Direct red 81 (DR-81) from single and binary solutions. The maximum capacity of this nanocomposite was reported to be 144.92 and 370.37 mg g^{-1} for DR-81 and Pb^{2+}, respectively [19].

The aim of this study was to synthesize and apply a novel sulfur-modified magnetic nanoparticle (SM-MNP) as an adsorbent for the removal of Pb^{2+} ions from aqueous solutions. The novel adsorbent was characterized by scanning electron microscopy (SEM), Fourier transform infrared (FTIR) spectroscopy, and thermogravimetric analysis (TGA). The kinetics and adsorption isotherms were investigated in order to evaluate adsorbent behavior. Finally applicability of the adsorbent for removal of lead from wastewater samples was investigated.

2. Materials and methods

2.1. Materials and reagents

All chemicals and reagents used were of analytical grade without any further purification. Isopropylamine ($(CH_3)_2CHNH_2$), carbon disulfide (CS_2), 3-(chloropropyl)trimethoxysilane ($Cl(CH_2)_3Si(OCH_3)_3$), lead nitrate ($Pb(NO_3)_2$), toluene ($C_6H_5CH_3$), methanol (CH_3OH), ethanol (C_2H_5OH), thiourea (CH_4N_2S), sodium hydroxide (NaOH) and hydrochloric acid (HCl) were purchased from the Merck (Darmstadt, Germany). Fe_3O_4 nanoparticles were prepared by a chemical co-precipitation method and were obtained from professor Yamini's research group [20]. Double-distilled deionized water was applied for preparing solutions. The stock solution of lead (1,000 mg L^{-1}) was prepared by dissolving the appropriate amounts of $Pb(NO_3)_2$ in doubly distilled water.

2.2. Instrumentation

A Varian (Mulgrave, Victoria, Australia) flame atomic absorption spectrometer (FAAS) model SpectrAA 110, with an air–acetylene flame was used for lead determinations. Absorbance measurements were carried out at 217.0 nm using lead hollow cathode lamp (from Varian) operated at 4.0 mA with deuterium background correction (at 10 mA). The instrumental parameters were used according to the manufacturer's recommendations. All measurements were based on peak height. The pH of the solutions was measured with a WTW pH meter (Inolab, Germany) which was supplied with a combined pH electrode. The morphology and surface structure of the adsorbents were studied using SEM (Model S-360, Cambridge Instruments Ltd., UK). The surface functional groups of samples were determined by FTIR spectroscopy (Vector 33 FT-IR, Bruker, Germany). Thermal stability of MNPs was studied by a Rheometric Scientific STA 1500 TGA instrument at a heating rate of 20°C min^{-1} in the temperature range of 25°C–700°C under nitrogen atmosphere.

2.3. Preparation of the adsorbent

For the preparation of new adsorbent, the magnetic Fe_3O_4 nanoparticles first functionalized by 3-(chloropropyl)trimethoxysilane. Briefly, 10.0 g of Fe_3O_4 nanoparticles were mixed with 6.5 mL of 3-(chloropropyl)trimethoxysilane and 50.0 mL of toluene. After 24 h, the mixture was filtered and washed three times with 20.0 mL toluene and two times with 20 mL ethanol; afterwards it was dried at vacuum oven under conditions of 50°C for 12 h. Next step is sulfur modification of the mixture. In real, the sulfur groups have a strong affinity binding for most heavy metals [21]. For this purpose, 5.0 mL carbon disulfide was slowly added to 1.64 mL isopropylamine under mild heat condition to form a white precipitate. Then, 0.54 g of this sulfur compound was dissolved in 10.0 mL methanol and afterwards 0.2 g of the magnetic Fe_3O_4 nanoparticles functionalized by 3-(chloropropyl)trimethoxysilane were added to it and kept at 65.0°C for 24 h (condenser condition). The final products were obtained after filtering and drying at 50.0°C in vacuum oven for 1 h and are hereafter referred to as SM-MNPs.

2.4. Adsorption procedure

Adsorption processes for all experiments were conducted in a 15 mL falcon tube containing 0.05 g of the adsorbent and 15 mL of lead solution with certain concentration and pH, which was shaken at room temperature for a given time. The pH of the lead solution was adjusted to the appropriate value with 0.1 mol L^{-1} HCl and NaOH. After adsorption, the suspensions of the adsorbent and Pb^{2+} in an aqueous solution were separated using a permanent magnet. The residual Pb^{2+} concentrations in the supernatant clear solutions were determined by FAAS using a calibration curve. All the adsorption experiments were carried out at ambient temperature (22°C–25°C).

The removal efficiency (E) and the adsorption capacity for lead uptake, q_e (mg g^{-1}), were determined as follows:

$$E(\%) = \frac{C_0 - C_e}{C_0} \times 100 \quad (1)$$

$$q_e = \frac{(C_0 - C_e) \times V}{m} \quad (2)$$

where q_e is the amount of the adsorbed Pb^{2+} on the NPs (mg g^{-1}; the equilibrium adsorption capacity), C_0 (mg L^{-1}) is the initial concentration of Pb^{2+}, C_e (mg L^{-1}) is the equilibrium concentration of the Pb^{2+} in the solution (mg L^{-1}), V is the volume of the Pb^{2+} solution (L) and m is the mass of the used NPs (g) [20].

2.5. Adsorption model fitting

The adsorption isotherm study was established for the adsorbent (0.05 g) in the 15 mL of lead solution with different initial concentrations of Pb^{2+} (10, 15, 20, 30, 35, 40, 45, and 50 mg L^{-1}) at optimal contact time. The pH of the solution in kinetics and sorption isotherm studies was adjusted to the optimal pH obtained in the pH effect study (pH = 3). The equilibrium adsorption of Pb^{2+} ion was evaluated according to Langmuir and Freundlich isotherms by Eqs. (3) and (4), respectively [22,23]:

$$q_e = q_m \frac{K_L C_e}{1 + K_L C_e} \quad (3)$$

$$q_e = K_F C_e^{1/n} \quad (4)$$

where C_e is Pb^{2+} concentration (mg L^{-1}) at equilibrium and q_e is amount adsorbed (mg g^{-1}), q_m is the maximum sorption capacity (mg g^{-1}). K_L (L mg^{-1}) and K_F (mg g^{-1})/(L $mg^{-1})^{-n}$ are the Langmuir and Freundlich sorption equilibrium constants, respectively. The Langmuir model is suitable for monolayer adsorption on a surface, whereas, Freundlich model is used on the basis of premising that stronger binding sites are occupied first [16].

2.6. Kinetic model fitting

The kinetics and adsorption isotherms were investigated. For the kinetics study experiment, 0.05 g of the adsorbent was added to 15 mL of a solution with the initial concentrations of Pb^{2+} adjusted to 1 mg L^{-1}. The mixture was shaken. Samples were withdrawn at different time intervals (5, 10, 20, 30, 45, and 60) and analyzed for the residual. Kinetics was analyzed using the Lagergren form of pseudo-first-order and pseudo-second-order models, as presented in Eqs. (5) and (6), respectively [12,22–24]:

$$\log(q_e - q_t) = \log q_e - k_1 t \quad (5)$$

$$\frac{t}{q_t} = \frac{1}{k_2 q_e^2} + \frac{t}{q_e} \quad (6)$$

where q_t and q_e (mg g^{-1}) are the amount adsorbed at time t (min) and equilibrium, respectively, and k_1 (min^{-1}) and k_2 [g(mg $min)^{-1}$] are the rate constants of pseudo-first-order and pseudo-second-order models, respectively.

2.7. Desorption study

Desorption study was carried out by 1 M solution of HCl containing 0.4 g thiourea as desorbing media. Initially, Pb^{2+} ions were adsorbed on the adsorbent from 15 mL solutions containing 1.0 mg L^{-1} of Pb^{2+} ions and then adsorbents were separated using an external magnetic field. Afterwards, adsorbents were stripped using 1 mL of 1 M solution of HCl containing 0.4 g thiourea by agitating at ambient temperature. The adsorbents were separated and supernatant's Pb^{2+} ion concentration was analyzed. The desorption efficiency was calculated using Eq. (7) [16]:

$$\text{Desorption efficiency (\%)} = \frac{\text{Released } Pb^{2+} \text{ concentration}}{\text{Initially sorbed } Pb^{2+} \text{ concentration}} \times 100 \quad (7)$$

2.8. Real water sample experiment

To study adsorbent performance in real water sample, the sorption experiment was performed with effluent wastewater from a battery factory wastewater treatment plant. Briefly, 0.05 g adsorbent was mixed with 15 mL of solution containing a mixture of Pb^{2+} ions and probable other solutes. The initial concentrations of Pb^{2+} in the test solution were 1.89 mg L^{-1}. The adsorption experiment was carried out at optimum condition obtained in this study and the sorption process was continued as described above.

3. Results and discussion

3.1. Characterization of the adsorbent

SEM micrograph of the adsorbent depicts the morphological characteristics favorable for metal adsorption. Fig. 1 shows a spherical morphology of the adsorbent (slightly agglomerated) with mean particle size of 100 nm.

The functional groups and surface properties of the adsorbent were confirmed by the FTIR spectra. Fig. 2 shows FTIR spectra of (A) the magnetic Fe_3O_4 nanoparticles functionalized by 3-(chloropropyl)trimethoxysilane, (B) the

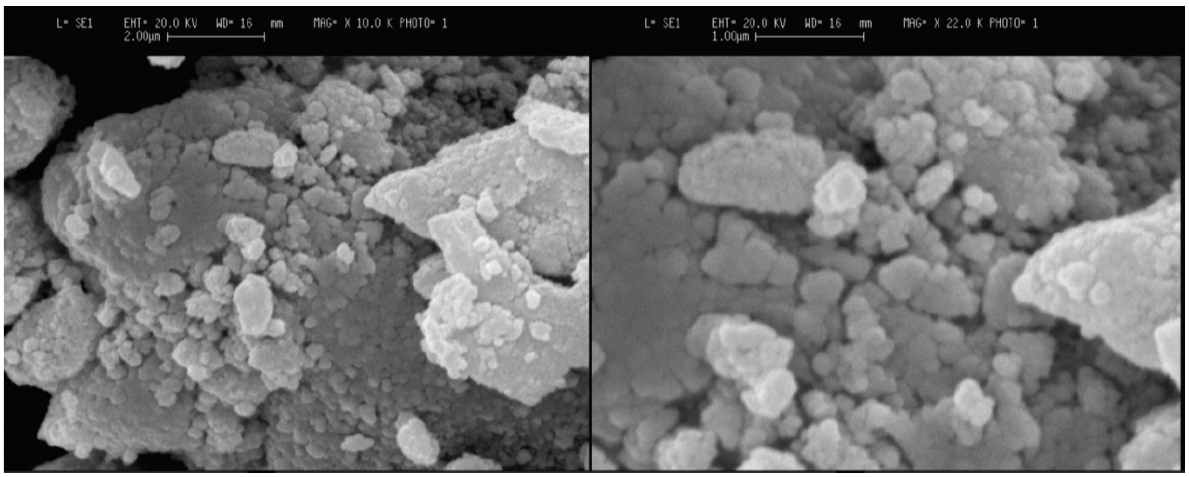

Fig. 1. SEM image of the adsorbent.

product of the reaction of carbon disulfide and isopropylamine, and (C) the synthesized final adsorbent. In the FTIR spectrum of the magnetic Fe_3O_4 nanoparticles functionalized by 3-(chloropropyl)trimethoxysilane (Fig. 2(A)), the bond at 1,399 cm^{-1} is related to C–Cl asymmetric stretching vibrations, and the peaks observed at 3,045, 3,143, 2,807, 593, 1,055, and 1,623 cm^{-1} could be assigned to the Si–O–H, asymmetric stretching vibrations of the C–H, Si–O, Si–O–Si vibrations, and O–H bending vibrations, respectively. In the FTIR spectrum of the product of the reaction of carbon disulfide and isopropylamine (Fig. 2(B)), the bonds at 1,486 and 2,582 cm^{-1} are related to C–N and S–H vibrations, respectively, and the peaks at 3,305 and 1,162 cm^{-1} could be assigned to the N–H deformation vibrations. In the FTIR spectrum of the synthesized final adsorbent (Fig. 2(C)), the peaks observed at 2,972, 1,556, and 596 cm^{-1} could be assigned to the asymmetric stretching vibrations of the C–H, C–N, and Si–O vibrations, respectively. Also, C–Cl vibrations were disappeared on the synthesized final adsorbent. This may be evidence that the adsorbent was successfully modified and functionalized. Observation of C–N and S–H vibrations in FTIR of the final adsorbent confirmed that there are good functional groups for interaction and removal of Pb^{2+} ions.

Fig. 3 shows TGA graph of the adsorbent. TGA curve of the adsorbent depicts that the weight loss over the temperature 25°C–200°C is about 6%. This might be because of the loss of residual water (physical and chemical water) in the sample. Then, the principle chains of polymer begin to decompose at about 200°C and the final temperature of degradation is around 300°C. Here, the weight loss is 40%. This evident confirmed that the surface of MNPs properly functionalized by alkyl chain containing sulfur group. Thus, the enhanced adsorption capability of the adsorbent would be expected because of the introduction of numerous functional groups on the adsorbent surface. At higher temperature (300°C–600°C), there is no significant change of weight. This implies that there is only Fe_3O_4 nanoparticles at this range of temperature and the presence of functional groups in/on the adsorbent are confirmed by TGA. This result is compatible with those of the other researches [22,25].

3.2. Effect of operating conditions on the adsorption of Pb^{2+}

The operating parameters such as initial solution pH, contact time, metal ion concentration, and other parameters can affect the surface characteristics of the adsorbent surface and its metal binding capacity [26]. Thus, a batch adsorption study was performed on the synthesized adsorbent to investigate the effect of these operating parameters on the removal efficiency and the adsorption capacity for lead uptake.

3.2.1. Effect of pH

Fig. 4 shows the initial solution pH dependency of Pb^{2+} ion removal from aqueous solutions by the adsorbent. The adsorption capacity was low at lower pH values (e.g., 30.0% at pH = 1). It seems that the positive charge on the adsorbent is generated in the acidic pH (low pH). So, there is an electrostatic repulsion between the adsorbent and Pb^{2+} ions in solution. The hydrogen ions instead of Pb^{2+}ions are placed into the adsorbent sites when the amount of hydrogen ions increases in solution, and so the removal efficiency is low [27]. The removal efficiency of Pb^{2+} was increased with increasing pH from 30.0% to 94.0% in the pH range of 1–2, then it was constant in the pH range of 2–4, and finally appeared to decrease at higher pH values. Therefore, the optimum pH selected to be 3 for the removal of Pb^{2+} from the aqueous solution. The increase in the Pb^{2+} adsorption on the adsorbent with increasing pH may be attributed to the surface charge and the availability of binding sites presented at the adsorbent surface [24,28]. The obtained results of the present study are approximately in line with the previous research findings [5,17].

3.2.2. Effect of adsorbent dosage

The effect of the adsorbent dosage on the removal efficiency was studied in the range of 0.01–0.1 g for a constant volume of Pb^{2+} solution (1 mg L^{-1}, 15 mL) at the initial solution pH of 3 and contact time of 5 min which is shown in Fig. 5. The removal efficiency increases as the dosage increases. In real, the removal efficiency increases, approaching 97.4% at a dosage of 0.05 g because the larger amount of adsorbent provides a greater surface area and more active adsorption

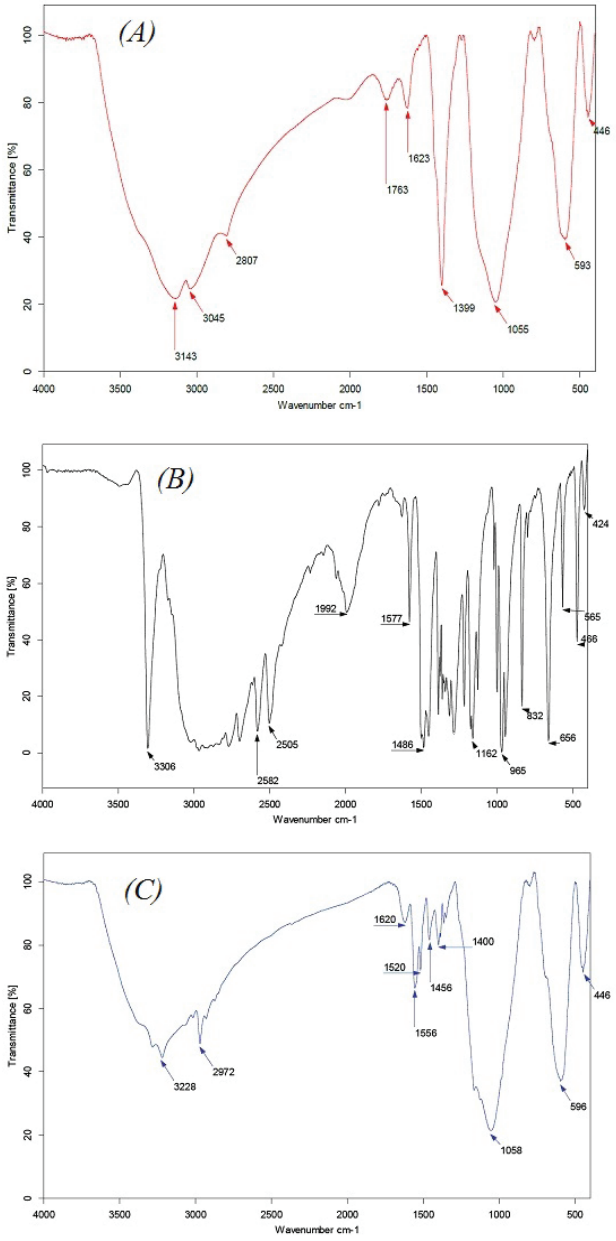

Fig. 2. FTIR spectra of (A) the magnetic Fe_3O_4 nanoparticles functionalized by 3-(chloropropyl)trimethoxysilane, (B) the product of the reaction of carbon disulfide and isopropylamine, and (C) the synthesized final adsorbent.

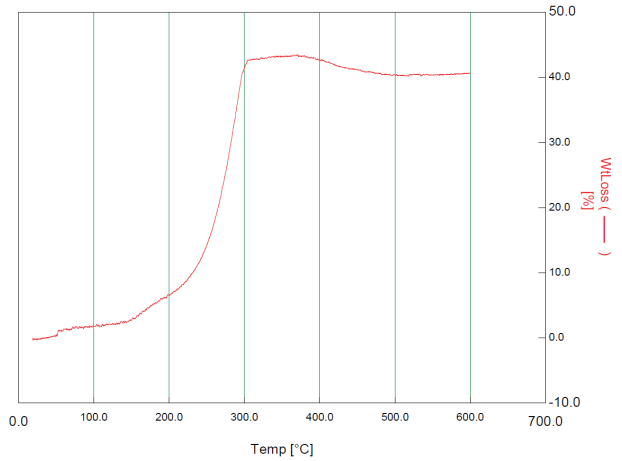

Fig. 3. Thermogravimetric analysis (TGA) of the adsorbent.

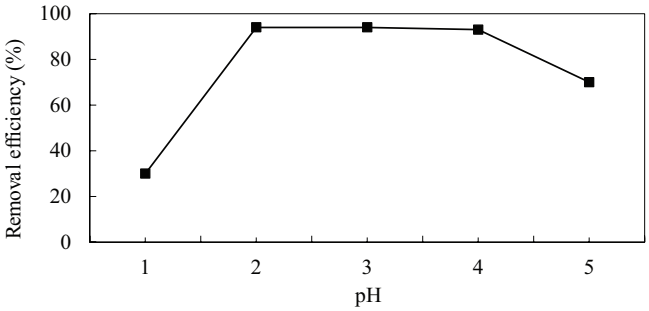

Fig. 4. The effect of initial solution pH on the removal efficiency of Pb^{2+} by the adsorbent.

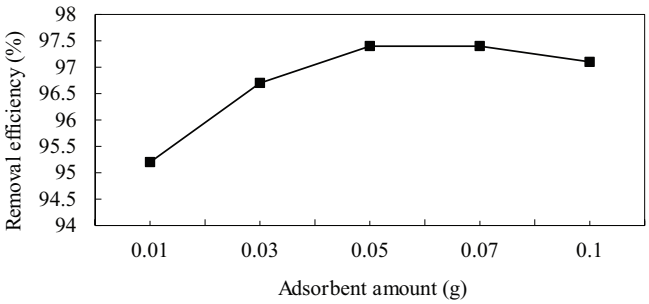

Fig. 5. The effect of the adsorbent dosage on the removal efficiency of Pb^{2+} by the adsorbent.

sites. However, excessive adsorbent in the solution may result in aggregation, which reduces the adsorbent's efficiency because the adsorption capacity is not fully saturated [5]. To ensure the maximum removal of Pb^{2+} and effective use of adsorbent, an adsorbent loading of 0.05 g was selected for subsequent adsorption experiments. The obtained result of this study has been seen in the previous researches [2,5].

3.2.3. Effect of contact time

Fig. 6 shows the effect of contact time on the removal efficiency of Pb^{2+} by the adsorbent. As this figure demonstrates, with increasing contact time, Pb^{2+} ion removal efficiency increases, because Pb^{2+} ions have more opportunities for contact with the adsorbent surface when time enhances. The rate of Pb^{2+} ions removal was fast in the beginning times (first 5 min) due to the larger surface area of the adsorbent available [27]. As time increases to 60 min, there are no big changes in removal efficiency due to the saturation of binding sites presented at the adsorbent surface. In real, the study of the removal efficiency of Pb^{2+} by the adsorbent revealed that the removal efficiency was approximately constant. For this reasons, the optimum contact time was selected as 5 min.

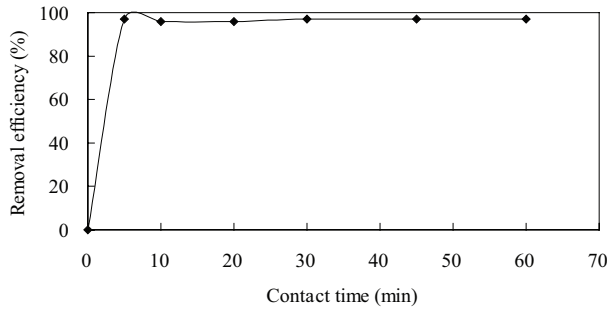

Fig. 6. The effect of contact time on the removal efficiency of Pb^{2+} by the adsorbent.

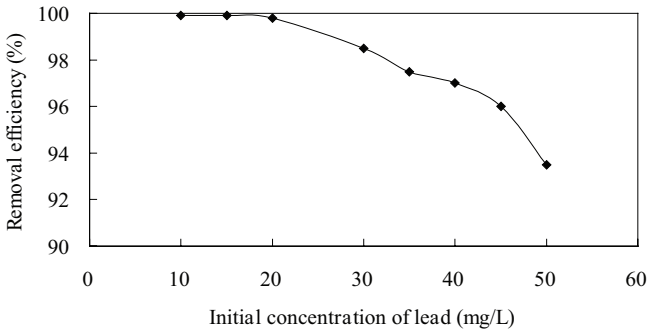

Fig. 7. The effect of initial Pb^{2+} concentration on the removal efficiency of Pb^{2+} by the adsorbent.

3.2.4. Effect of initial concentration of Pb^{2+}

The effect of initial Pb^{2+} concentration on the removal efficiency of Cd^{2+} by the adsorbent is shown in Fig. 7. According to Fig. 7, with increasing Pb^{2+} concentration of 10–20 mg L^{-1}, the removal efficiency is approximately constant; and then appeared to decrease at higher initial Pb^{2+} concentration values.

An enhanced ratio of initial number of Pb^{2+} ions to the available surface area resulted in high concentration; hence fractional adsorption relies on initial concentration. For a given amount of the adsorbent (0.05 g of the adsorbent) the total number of available adsorption active sites is constant thereby adsorbing almost the same amount of Pb^{2+}, therefore, a decrease in the removal of Pb^{2+} was resulted to an increase in initial concentration of Pb^{2+} due to the saturation of binding sites presented at the adsorbent surface [27,29].

3.3. Adsorption isotherms

Equilibrium isotherms are applied to describe the experimental adsorption data. The parameters obtained from the different models provide important information on the adsorption mechanisms and the surface properties and affinities of the adsorbent [20].

The Langmuir and Freundlich models were used to determine the adsorption isotherm for Pb^{2+} removal by synthesized adsorbent that the obtained results are presented in Table 1. In the Langmuir model, a plot of C_e/q_e vs. C_e should indicate a straight line of slope $1/q_m$ and an intercept of $1/(K_L.q_m)$ (Fig. 8(A)). K_F and n are empirical constants of the Freundlich model which indicate the adsorption capacity and adsorption intensity, and can be calculated from the slope and intercept of the linear plot (Fig. 8(B)). The correlation coefficient showed good positive evidence on the adsorption of Pb^{2+} onto the adsorbent (R^2 = 0.984) follows the Langmuir isotherm. The maximum monolayer capacity q_m and K_L the Langmuir constant were calculated from the Langmuir as 14.03 mg g^{-1} and 8.39 L mg^{-1}, respectively.

Based on the correlation coefficient (R^2), the fit of the data for Pb^{2+} adsorption onto the adsorbent suggests that the Langmuir model (R^2 = 0.984) gave better fitting than that of the Freundlich model (R^2 = 0.944). It may also be concluded from these data that the surface of the adsorbent is made up of homogenous adsorption patches than heterogeneous adsorption patches [20,30]. The exponent n of 3.81 is in the range of 1–10, indicating a favorable adsorption [19,31]. These results indicate that the adsorbent developed in the current study has great potential for the removal of Pb^{2+} from contaminated water.

Table 1
Langmuir and Freundlich model correlation coefficients and constants for adsorption of Pb^{2+} on the absorbent at ambient temperature

Model	Parameters		
Langmuir	q_m (mg g^{-1})	K_L (L mg^{-1})	R^2
	14.03	8.39	0.984
Freundlich	K_F (mg g^{-1})/(L $mg^{-1})^{-n}$	n	R^2
	10.74	3.81	0.944

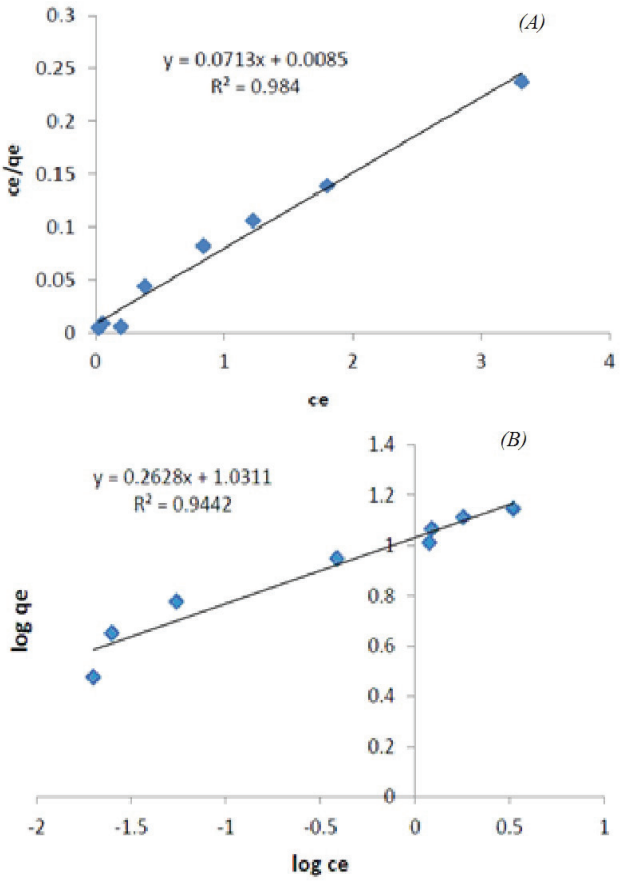

Fig. 8. Langmuir (A) and Freundlich (B) isotherm models for the adsorption of Pb^{2+} on the adsorbent.

3.4. Adsorption kinetics

To study the rate of adsorption [12], its mechanism, and its potential rate-controlling steps that include mass transport and chemical reaction processes [21], the kinetic data were fitted by the Lagergren form of pseudo-first-order and pseudo-second-order models (Fig. 9). The fitting parameters from the two models are listed in Table 2.

It can be seen that the R^2 value of the pseudo-second-order model (0.9999) was higher than those of the Lagergren form of pseudo-first order (0.0504). This result indicated that the Pb^{2+} adsorption processes followed a second-order type kinetic reaction, which suggests that the adsorption rate in the solutions was probably limited by chemisorption, and the adsorption probably takes place via surface complexation reactions at specific sorption sites [21,32]. In the other words, it suggested the multi-step process involving sorption on the external surface and diffusion into the interior of adsorbent, or the process could be chemisorption through valence force by sharing or by exchange of electron between the adsorbent and Pb^{2+} ions [12].

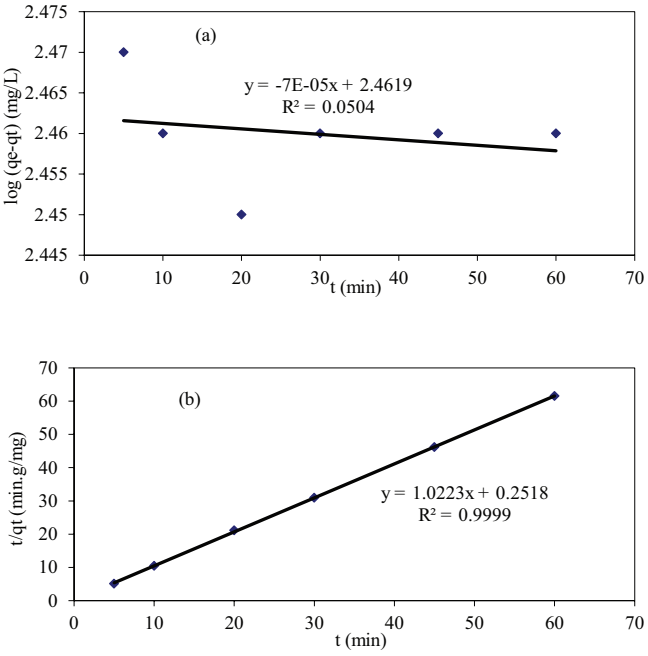

Fig. 9. Sorption kinetics fitted by (A) Lagergren form of pseudo-first-order and (B) pseudo-second-order of Pb^{2+} onto the adsorbent in solution.

3.5. Adsorption mechanism

Lead is soft metal in nature and it has trend to bind with soft (sulfur) and intermediate soft (nitrogen) functional groups at the suitable pH range. Therefore, interaction of sulfur and nitrogen groups on the surface of the adsorbent with Pb^{2+} ions can be the main adsorption mechanism.

3.6. Desorption and regeneration

From an economical point of view and the feasibility study of adsorption process, the desorption efficiency and regeneration potential of a sorbent are key evaluation factors [2,33]. Desorption studies were carried out by 1 M solution of HCl containing 0.4 g thiourea as desorbing media. Result indicated that desorption efficiency was approximately 98%. Such desorption ability of the adsorbent can diminish operation costs and may indicate industrial applicability [33].

3.7. Removal performance of the adsorbent in real wastewater samples

To study adsorbent performance in real wastewater sample, the sorption experiment was performed with effluent wastewater from a battery factory wastewater treatment plant under optimum conditions. Result showed that the removal efficiency was 76.72%. The removal efficiency for real water sample is lower than that of synthetic water sample due to the presence of other solutes in real sample and saturation of active sites of adsorbent with them.

4. Conclusion

A novel SM-MNP was applied as an adsorbent for the removal of Pb^{2+} ions from aqueous solutions. SEM micrograph of the adsorbent depicted the morphological characteristics favorable for metal adsorption. The functional groups and surface properties of the adsorbent were confirmed by the FTIR spectra and TGA. Observation of C–N and S–H vibrations in FTIR of the final adsorbent confirmed that there are good functional groups for interaction and removal of Pb^{2+} ions. The optimum pH, adsorbent amount, contact time, and initial concentration of Pb^{2+} in the batch adsorption studies were 3, 0.05 g, 5 min, and 10–20 mg L^{-1}, respectively. The equilibrium data fitted the Langmuir isotherm model better than the Freundlich isotherm model, and they were well explained in terms of pseudo-second-order kinetics. The maximum monolayer capacity q_m and K_L the Langmuir constant were calculated from the Langmuir as 14.03 mg g^{-1}

Table 2
Kinetic models and obtained parameters for adsorption of Pb^{2+} on the adsorbent

	Model	Obtained equation	Calculated values
Lagergren form of pseudo-first-order	$\log(q_e - q_t) = \log q_e - k_1 t$	$Y = -7 \times 10^{-5}X + 2.4619$	$R^2 = 0.0504$ $k_1 = 7 \times 10^{-5}$ min^{-1} $q_e = 289.66$ mg^{g-1}
Pseudo-second-order	$\frac{t}{q_t} = \frac{1}{k_2 q_e^2} + \frac{t}{q_e}$	$Y = 1.0223X + 0.2518$	$R^2 = 0.9999$ $k_2 = 4.1512$ g mg^{-1} min^{-1} $q_e = 0.9781$ mg g^{-1}

and 8.39 L mg^{-1}, respectively. The desorption efficiency was approximately 98% which this desorption ability of the adsorbent can diminish operation costs and may indicate industrial applicability. Under optimum conditions, the applicability of the adsorbent in real wastewater sample was investigated by the removal of lead from effluent wastewater from a battery factory wastewater treatment plant in which the removal efficiency was 76.72%. The removal efficiency for real water sample is lower than that of synthetic water sample due to the presence of other solutes in real sample and saturation of active sites of adsorbent with them. In the future, this SM-MNP should be tested for the removal of other heavy metals and/or contaminants from aqueous solutions.

References

[1] H.T. Fan, J.B. Wu, X.L. Fan, D.S. Zhang, Z.J. Su, F. Yan, T. Sun, Removal of cadmium(II) and lead(II) from aqueous solution using sulfur-functionalized silica prepared by hydrothermal-assisted grafting method, Chem. Eng. J., 198–199 (2012) 355–363.

[2] D. Afzali, M. Fayazi, Deposition of MnO_2 nanoparticles on the magnetic halloysite nanotubes by hydrothermal method for lead(II) removal from aqueous solutions, J. Taiwan Inst. Chem. Eng., 63 (2016) 421–429.

[3] S. Jafarinejad, Petroleum Waste Treatment and Pollution Control, 1st ed., Elsevier Inc., Butterworth-Heinemann, USA, 2016.

[4] R. Singh, N. Gautam, A. Mishra, R. Gupta, Heavy metals and living systems: an overview, Indian J. Pharmacol. 43 (2011) 246–253.

[5] J. Lu, R.N. Jin, C. Liu, Y.F. Wang, X. Ouyang, Magnetic carboxylated cellulose nanocrystals as adsorbent for the removal of Pb(II) from aqueous solution, Int. J. Biol. Macromol., 93 (2016) 547–556.

[6] J.M. Bai, X.P. Liu, Heavy metal pollution in surface soils of Pearl River Delta China (Retracted article. See vol. 187, p. 112, 2015), Environ. Monit. Assess., 186 (2014) 8051–8061.

[7] X.M. Li, Z. Wei, D.B. Wang, Y. Qi, J.B. Cao, Y. Xiu, T.T. Shen, G.M. Zeng, Removal of Pb(II) from aqueous solutions by adsorption onto modified areca waste: kinetic and thermodynamic studies, Desalination, 258 (2010) 148–153.

[8] W. Lo, H. Chua, K.H. Lam, S.P. Bi, A comparative investigation on the biosorption of lead by filamentous fungal biomass, Chemosphere, 39 (1999) 2723–2736.

[9] A. Ayar, D. Sert, N. Akin, The trace metal levels in milk and dairy products consumed in middle Anatolia-Turkey, Environ. Monit. Assess., 152 (2009) 1–12.

[10] C.C. Yu, J.L. Lin, D.T. Lin-Tan, Environmental exposure to lead and progression of chronic renal diseases: a four-year prospective longitudinal study, J. Am. Soc. Nephrol., 15 (2004) 1016–1022.

[11] J.O. Duruibe, M.O.C. Ogwuegbu, J.N. Egwurugwu, Heavy metal pollution and human biotoxic effects, Int. J. Phys. Sci., 2 (2007) 112–118.

[12] D. Singh, R.K. Gautam, R. Kumar, B.K. Shukla, V. Shankar, V. Krishna, Citric acid coated magnetic nanoparticles: synthesis, characterization and application in removal of Cd(II) ions from aqueous solution, J. Water Process Eng., 4 (2014) 233–241.

[13] N.A. Abdelwahab, N.S. Ammar, H.S. Ibrahim, Graft copolymerization of cellulose acetate for removal and recovery of lead ions from wastewater, Int. J. Biol. Macromol., 79 (2015) 913–922.

[14] A. Afkhami, R. Norooz-Asl, Removal, preconcentration and determination of Mo(VI) from water and wastewater samples using maghemite nanoparticles, Colloids Surf., A, 346 (2009) 52–57.

[15] S. Yavari, N.M. Mahmodi, P. Teymouri, B. Shahmoradi, A. Maleki, Cobalt ferrite nanoparticles: preparation, characterization and anionic dye removal capability, J. Taiwan Inst. Chem. Eng., 59 (2016) 320–329.

[16] S. Rajput, C.U. Pittman Jr., D. Mohan, Magnetic magnetite (Fe_3O_4) nanoparticle synthesis and applications for lead (Pb^{2+}) and chromium (Cr^{6+}) removal from water, J. Colloid Interface Sci., 468 (2016) 334–346.

[17] R. Verma, A. Asthana, A.K. Singh, S. Prasad, Md. A.B.H. Susan, Novel glycine-functionalized magnetic nanoparticles entrapped calcium alginate beads for effective removal of lead, Microchem. J., 130 (2016) 168–178.

[18] L.P. Lingamdinne, Y.Y. Chang, J.K. Yang, J. Singh, E.H. Choi, M. Shiratani, J.R. Koduru, P. Attri, Biogenic reductive preparation of magnetic inverse spinel iron oxide nanoparticles for the adsorption removal of heavy metals, Chem. Eng. J., 307 (2017) 74–84.

[19] M.H. Beyki, M. Shirkhodaie, M.A. Karimi, M.J. Aghagoli, F. Shemirani, Green synthesized Fe_3O_4 nanoparticles as a magnetic core to prepare poly 1,4 phenylenediamine nanocomposite: employment for fast adsorption of lead ions and azo dye, Desal. Wat. Treat., 57 (2016) 28875–28886.

[20] S. Shariati, M. Faraji, Y. Yamini, A.A. Rajabi, Fe_3O_4 magnetic nanoparticles modified with sodium dodecyl sulfate for removal of safranin O dye from aqueous solutions, Desalination, 270 (2011) 160–165.

[21] A. Chen, C. Shang, J. Shao, Y. Lin, S. Luo, J. Zhang, H. Huang, M. Lei, Q. Zeng, Carbon disulfide-modified magnetic ion-imprinted chitosan-Fe(III): a novel adsorbent for simultaneous removal of tetracycline and cadmium, Carbohydr. Polym., 155 (2017) 19–27.

[22] Y. Huang, A.N. Fulton, A.A. Keller, Simultaneous removal of PAHs and metal contaminants from water using magnetic nanoparticle adsorbents, Sci. Total Environ., 571 (2016) 1029–1036.

[23] G. Zhao, X. Wu, X. Tan, X. Wang, Sorption of heavy metal ions from aqueous solutions: a review, Open Colloid Sci. J., 4 (2011) 19–31.

[24] R.R. Shan, L.G. Yan, K. Yang, Y.F. Hao, B. Du, Adsorption of Cd(II) by Mg–Al–CO_3- and magnetic Fe_3O_4/Mg–Al–CO_3-layered double hydroxides: kinetic, isothermal, thermodynamic and mechanistic studies, J. Hazard. Mater., 299 (2015) 42–49.

[25] S. Asgari, Z. Fakhari, S. Berijani, Synthesis and characterization of Fe_3O_4 magnetic nanoparticles coated with carboxymethyl chitosan grafted sodium methacrylate, J. Nanostruct., 4 (2014) 55–63.

[26] V.K. Gupta, A. Nayak, Cadmium removal and recovery from aqueous solutions by novel adsorbents prepared from orange peel and Fe_2O_3 nanoparticles, Chem. Eng. J., 180 (2012) 81–90.

[27] M.H. Ehrampoush, M. Miria, M.H. Salmani, A.H. Mahvi, Cadmium removal from aqueous solution by green synthesis iron oxide nanoparticles with tangerine peel extract, J. Environ. Health Sci. Eng., 13 (2015) 84.

[28] D. Zhao, G. Sheng, J. Hu, C. Chen, X. Wang, The adsorption of Pb(II) on Mg_2Al layered double hydroxide, Chem. Eng. J., 171 (2011) 167–174.

[29] B. Kakavandi, A.J. Jonidi, R.K. Rezaei, S. Nasseri, A. Ameri, A. Esrafily, Synthesis and properties of Fe_3O_4-activated carbon magnetic nanoparticles for removal of aniline from aqueous solution: equilibrium, kinetic and thermodynamic studies, J. Environ. Health Sci. Eng., 10 (2013) 19.

[30] M. Faraji, Y. Yamini, E. Tahmasebi, A. Saleh, F. Nourmohammadian, Cetyltrimethylammonium bromide-coated magnetite nanoparticles as highly efficient adsorbent for rapid removal of reactive dyes from the textile companies' wastewaters, J. Iran. Chem. Soc., 7 (2010) S130–S144.

[31] H. Li, D.L. Xiao, H. He, R. Lin, P.L. Zuo, Adsorption behavior and adsorption mechanism of Cu(II) ions on amino-functionalized magnetic nanoparticles, Trans. Nonferrous Met. Soc. China, 23 (2013) 2657–2665.

[32] Y. Ma, Q. Zhou, S. Zhou, W. Wang, J. Jin, J. Xie, A bifunctional adsorbent with high surface area and cation exchange property for synergistic removal of tetracycline and Cu^{2+}, Chem. Eng. J., 258 (2014) 26–33.

[33] G.A. Mahmoud, Adsorption of copper(II), lead(II), and cadmium(II) ions from aqueous solution by using hydrogel with magnetic properties, Monatsh. Chem., 144 (2013) 1097–1106.